Oil & Natural Gas Technology

DOE Award No.: DE-FC26-06NT42960

Quarterly Progress Report

Reporting Period: January-March, 2008

Detection and Production of Methane Hydrate

Submitted by:
Rice University
University of Houston
George J. Hirasaki
Department of Chemical and Biomolecular Engineering
Rice University – MS 362
6100 Main St.
Houston, TX 77251-1892
Phone: 713-348-5416; FAX: 713-348-5478; Email: gjh@rice.edu

Prepared for:
United States Department of Energy
National Energy Technology Laboratory

April, 2008

Office of Fossil Energy

Table of Contents

Disclaimer

Executive Summary

Task 5: Carbon Inputs and Outputs to Gas Hydrate System

Models concerning the abundance and distribution of gas hydrate in marine sediment require constraints on carbon inputs and outputs, fluid flow and temporal evolution. We have now generated a series of sediment and pore water data sets that can be used to constrain our models.

Task 6: Numerical Models for Quantification of Hydrate and Free Gas Accumulations

Subtask 6.1 Model Development

Our first student, Gaurav Bhatnagar has completed his PhD requirements and begun employment with Shell. A new PhD student, Sayantan Chatterjee is continuing the model development and illustrates the effect of a vertical fracture or a high-permeability on focusing fluid flow and enhancing hydrate and free gas accumulation.

Subtask 6.3 Compositional Effects

Second year PhD student, Guangsheng Gu illustrates compositional effects on the transition from hydrate saturation to gas saturation. When two hydrocarbon components are present, three phases can co-exist and the transition zone may be hundreds of meters thick. A gradual transition will reduce the gradient in acoustic impedance and may weaken or even eliminate a BSR at the base of the hydrate stability zone.

Task 7: Analysis of Production Strategy

In this work, we are considering injection of warm water and depressurization for production from Class 2 hydrate reservoirs. The source of warm water could be a nearby oil reservoir or an underlying water aquifer. Gas production from a hydrate reservoir is studied through numerical simulation.

Task 8: Seafloor and Borehole Stability

We are using published literature to constrain the mechanical properties of hydrate bearing sediments to understand deformation, flow, and strength properties that affect regional seafloor stability and local borehole stability. This includes culling the literature to assess what data have been compiled, the method of measurement, and identifying where strengths and gaps exist. Secondly we are running laboratory experiments on fine-grained materials from hydrate settings but in the absence of hydrate. These experiments will set the baseline parameters (permeability, compressibility, strength) for model inputs that are the modified according to hydrate saturation. We are also coupling the physical properties into basin-scale fluid flow models that simulate sediment accumulation and conditions that can lead to slope instability.

Task 9: Geophysical Imaging of Gas Hydrate and Free Gas Accumulations

For this task in particular, and others in general, we have successfully initiated collaboration with National Institute of Oceanography (NIO), India. We intend to demonstrate geophysical imaging with multichannel seismic data from the Krishna-Godavari (K-G) basin in the Indian east coast. NIO scientists are tentatively scheduled to visit Rice University in the first week of June.

Background

A. Objective

This project seeks to understand regional differences in gas hydrate systems from the perspective of as an energy resource, geohazard, and long-term climate influence. Specifically, the effort will: (1) collect data and conceptual models that targets causes of gas hydrate variance, (2) construct numerical models that explain and predict regional-scale gas hydrate differences in 2- and 3-dimensions with minimal "free parameters", (3) simulate hydrocarbon production from various gas hydrate systems to establish promising resource characteristics, (4) perturb different gas hydrate systems to assess potential impacts of hot fluids on seafloor stability and well stability, and (5) develop geophysical approaches that enable remote quantification of gas hydrate heterogeneities so that they can be characterized with minimial costly drilling. Our integrated program takes advantage of the fact that we have a close working team comprised of experts in distinct disciplines.

The expected outcomes of this project are improved exploration and production technology for production of natural gas from methane hydrates and improved safety through understanding of seafloor and well bore stability in the presence of hydrates.

B. Scope of Work

The scope of this project is to more fully characterize, understand, and appreciate fundamental differences in the amount and distribution of gas hydrate and how this affects the production potential of a hydrate accumulation in the marine environment. The effort will combine existing information from locations in the ocean that are dominated by low permeability sediments with small amounts of high permeability sediments, one permafrost location where extensive hydrates exist in reservoir quality rocks and other locations deemed by mutual agreement of DOE and Rice to be appropriate. The initial ocean locations are Blake Ridge, Hydrate Ridge, Peru Margin and GOM. The permafrost location is Mallik. Although the ultimate goal of the project is to understand processes that control production potential of hydrates in marine settings, Mallik will be included because of the extensive data collected in a producible hydrate accumulation. To date, such a location has not been studied in the oceanic environment. The project will work closely with ongoing projects (e.g. GOM JIP and offshore India) that are actively investigating potentially economic hydrate accumulations in marine settings.

The overall approach is fivefold: (1) collect key data concerning hydrocarbon fluxes which is currently missing at all locations to be included in the study, (2) use this and existing data to build numerical models that can explain gas hydrate variance at all four locations, (3) simulate how natural gas could be produced from each location with different production strategies, (4) collect new sediment property data at these locations that are required for constraining fluxes, production simulations and assessing sediment stability, and (5) develop a method for remotely quantifying heterogeneities in gas hydrate and free gas distributions. While we generally restrict our efforts to the locations where key parameters can be measured or constrained, our ultimate aim is to make our efforts universally applicable to any hydrate accumulation.

Task 5: Carbon Inputs and Outputs to Gas Hydrate Systems

Subtask 5.1a: Constrain organic carbon inputs using iodine

The sedimentary input of labile organic carbon over time contributes significantly to the amount and distribution of gas hydrate in marine sediment (e.g., Bhatnager et al., 2007). We have generated a series of iodine profiles for sediment and pore waters through several gas hydrate systems (Blake Ridge, Peru Margin, Gulf of Mexico, Japan Sea) as well as several "reference sites" without gas hydrate. Iodine concentrations in sediment from Blake Ridge and Peru Margin are extremely high, and these amounts and profiles (**Fig. 5.1-1**) have a fairly straightforward interpretation. Organic carbon lands on the seafloor with iodine. During burial, iodine is released from the organic carbon, contributing to iodide in pore water. This iodide moves upward toward the seafloor, by diffusion, advection or both. Here, it is converted to iodate and re-scavenged by organic carbon. The consequence is a system where the amount of iodine in pore waters is proportional to carbon input and fluid dynamics over time. The concentrations are extreme for Blake Ridge and Peru Margin because they have received very large fluxes of organic carbon (and iodine) over long time intervals. We are continuing to write the results of our iodine work and expect to have a manuscript submitted by the end of summer.

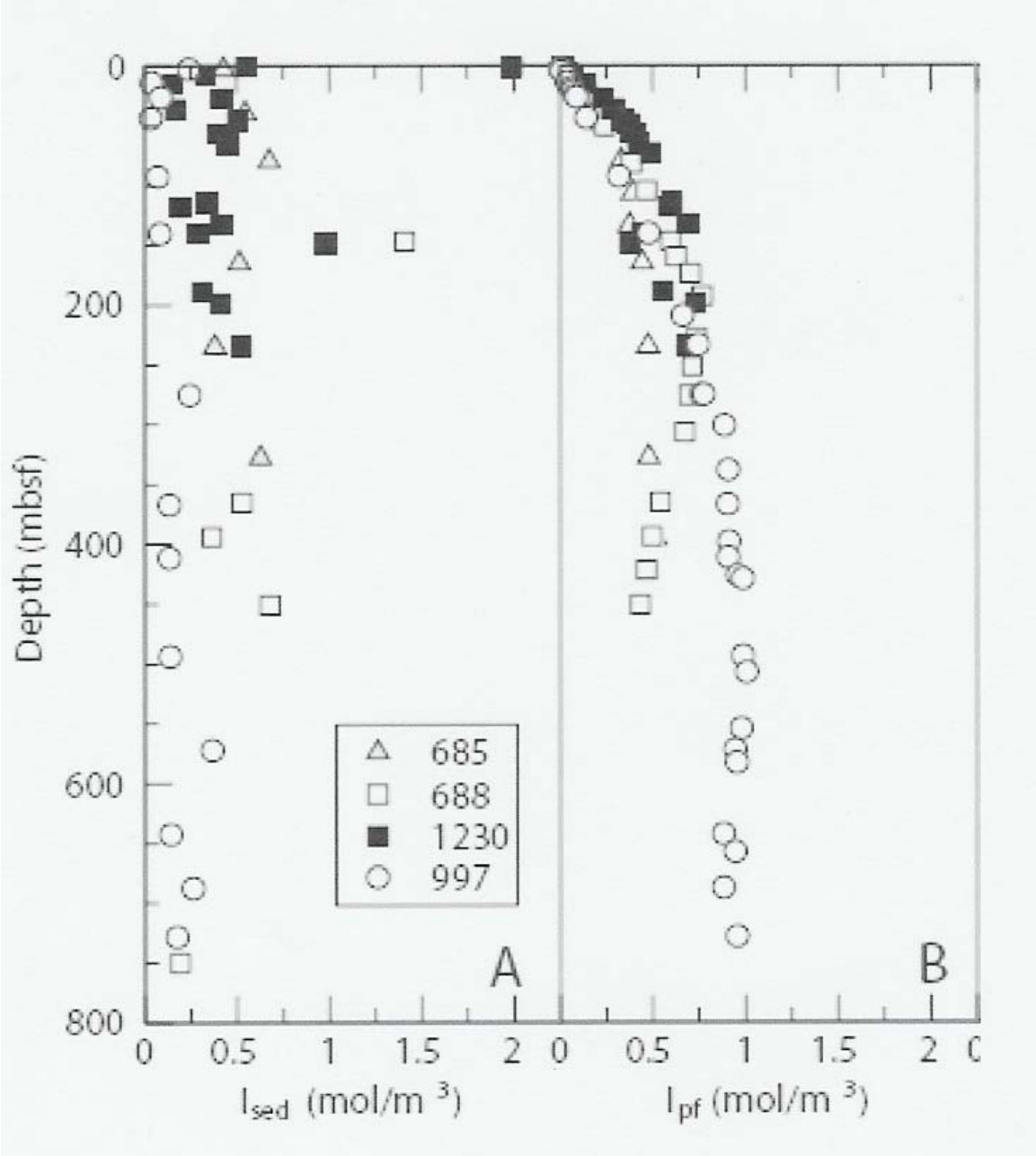

Figure 5.1-1: Sediment and pore water iodine concentrations in drill holes from Peru Margin and Blake Ridge.

Subtask 5.2a: Constrain methane outputs using metals and carbon isotopes

The depth of the sulfate-methane transition (SMT) should be related to amount and distribution of gas hydrate, provided that (1) essentially all sulfate is consumed by anaerobic oxidation of methane (AOM), and (2) the system has been at steady-state conditions for considerable time (e.g., Bhatnager et al., 2008). We are trying to constrain these by examining carbon fluxes across the SMT and profiles of Ca and Ba in shallow sediment.

We have now collected or obtained all data relevant to understanding carbon fluxes in shallow sediment at ODP Site 1230 on the Peru Margin. This data includes gas abundances, sediment and pore water C, Ca, Mg, Sr and Ba concentrations, and carbon isotopes of dissolved bicarbonate and solid carbonate. We are currently putting together box models for this data, like we did for the Japan Sea cores (Snyder et al., 2007). The preliminary interpretation is that almost all sulfate is consumed via AOM.

Conclusions:

We have now analyzed iodine, carbon phases and metals in sediment from several drill holes. In general, the iodine profiles provide a first order constraint on the input of organic carbon to gas hydrate systems; the carbon phases and metals in shallow sediment provide a first order constraint on the output of methane from gas hydrate systems.

Future Work:

We will generate several more metal profiles in an effort to develop a uniform view of how methane escape via AOM impacts shallow sediment. We then use this data to evaluate our models concerning the abundance and distribution of gas hydrate in marine sediment.

Task 6: Numerical Models for Quantification of Hydrate and Free Gas Accumulations

Subtask 6.1: Model Development

Natural gas hydrate system is complex and heterogeneous and includes some additional features in addition to our previous 1-D model. Fractured systems, parallel or dipping sediment beds are common heterogeneities and fluid flow within natural gas hydrate systems are predominated primarily in these local fractures and high permeability sand layers, resulting in concentrated hydrate deposits. To incorporate these additional features and simulate realistic geologic systems, we extended our existing 1-D model to 2-D model (Bhatnagar, 2008).

Gas hydrate systems with fractures

Fractures can dominate focused fluid flow in natural gas systems, acting as high permeability conduits causing localized concentrations of hydrate and free gas within these fracture networks. We simulate vertical fractures in our model, where we assign average vertical permeability in different grid blocks in a single column throughout our simulation domain as shown below.

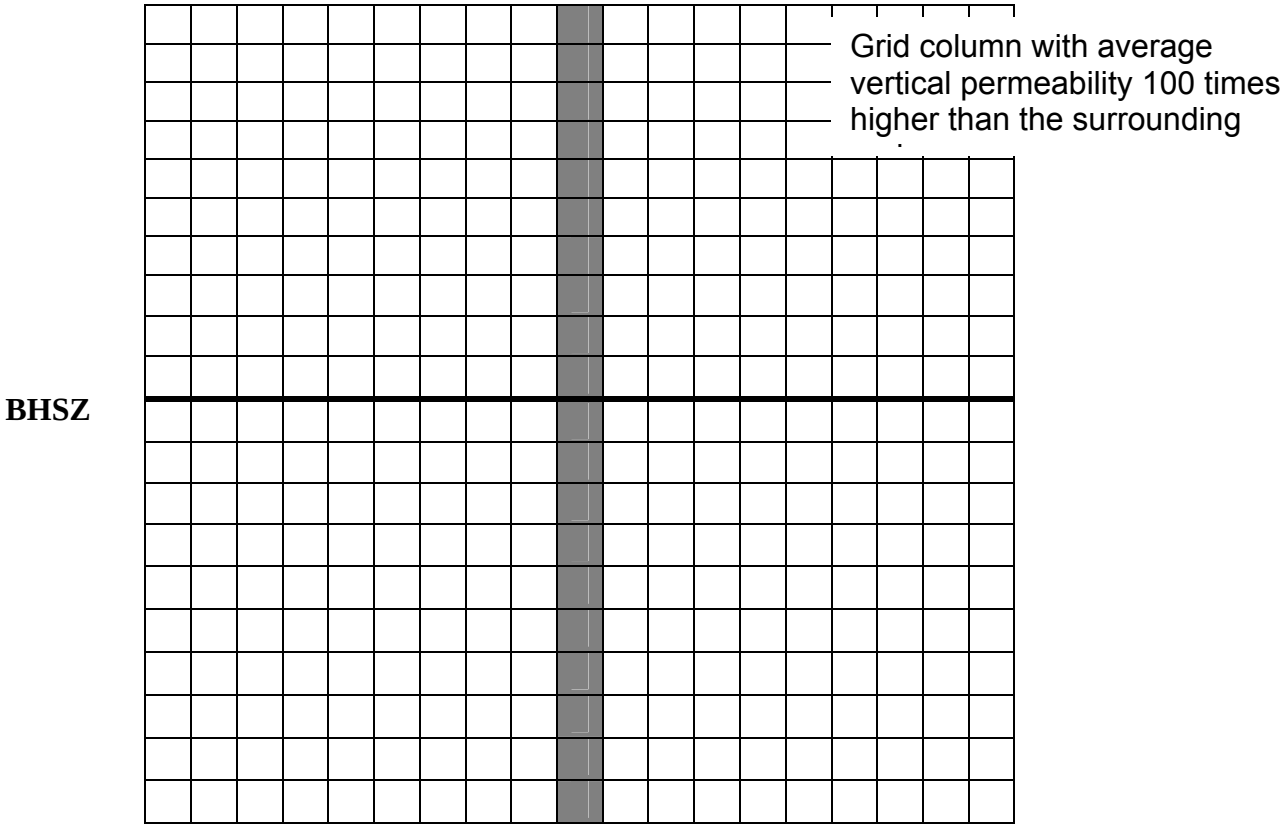

Figure 6.1-1: Permeability map showing initial location of a single high permeability vertical fracture

We introduce a single fracture and follow the transient gas hydrate and free gas accumulation with sedimentation. In our first case, we model a stationary fracture which does not move down with sedimentation. The vertical

permeability is 100 times higher than the surrounding region. The primary transport parameters are assigned as follows: Pe_1=0.1, Da=10, β=6, γ=9, η=6/9, $N_{t\varphi}$=1. Seafloor parameters, relative permeabilities, capillary pressure and physical properties of water, hydrate and free gas are the same as we used in our 1-D model. We report the results at different transient states. The location of the fracture is represented by a set of dashed lines. We clearly observe a high focused flow along the high permeability conduit along the fracture. Buoyant free gas migrates upwards and gets sealed by the low permeability hydrate layer at the base of hydrate stability zone (BHSZ). In a later case, we simulate a case, where the fracture moves down with sedimentation. With passage of time, as the fracture moves out of the gas hydrate stability zone (GHSZ), hydrate distribution becomes more uniform along the lateral direction. Free gas saturation also reaches a peak value and spreads out laterally as the fracture is buried in longer times. Thus, we study the presence of vertical fractures with higher average permeability which significantly affects gas hydrate and free gas distribution by focusing fluid flow along these fractures.

Dimensionless distance is defined with characteristic depth to the base of the GHSZ L_t

$$\tilde{z} = \frac{z}{L_t} \quad , \quad \tilde{x} = \frac{x}{L_t}$$

Dimensionless time is defined by a combination of L_t and the methane diffusivity D_m

$$\tilde{t} = \frac{t}{L_t^2 / D_m}$$

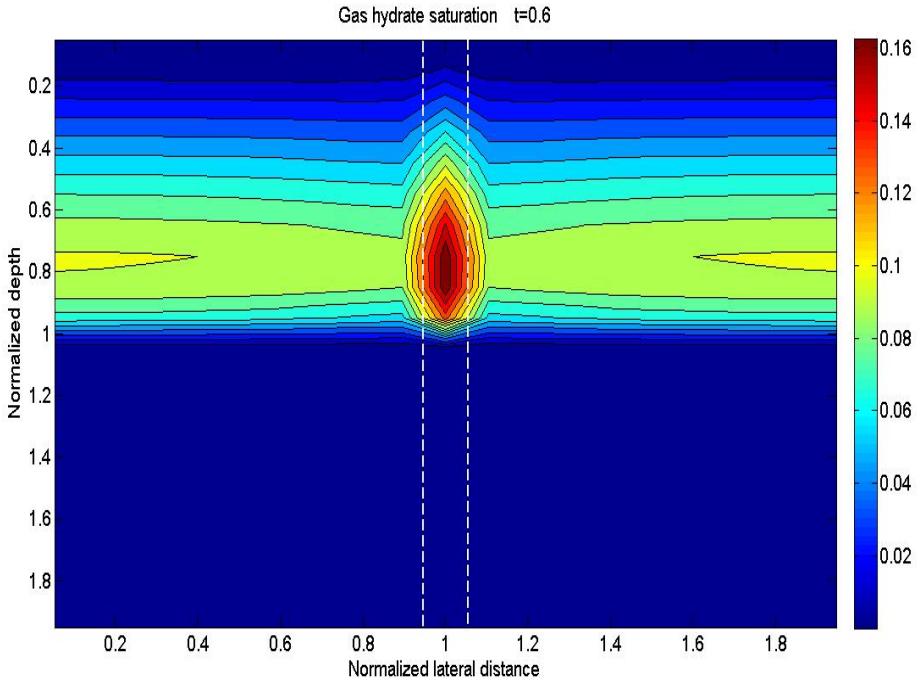

Figure: Gas hydrate saturation contours at dimensionless time t=0.6 for a stationary fracture

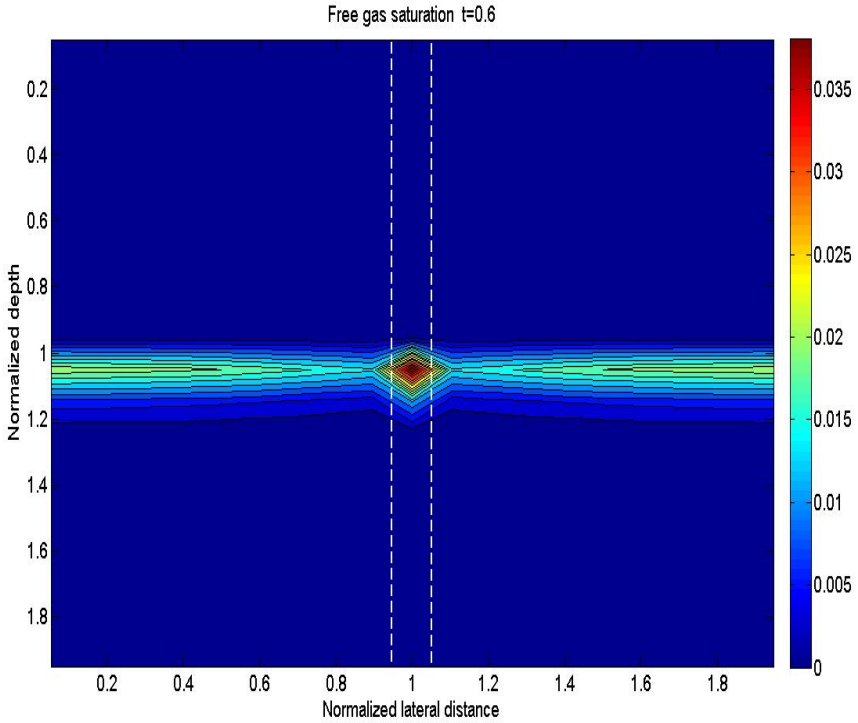

Figure: Free gas saturation contours at dimensionless time t=0.6 for a stationary fracture

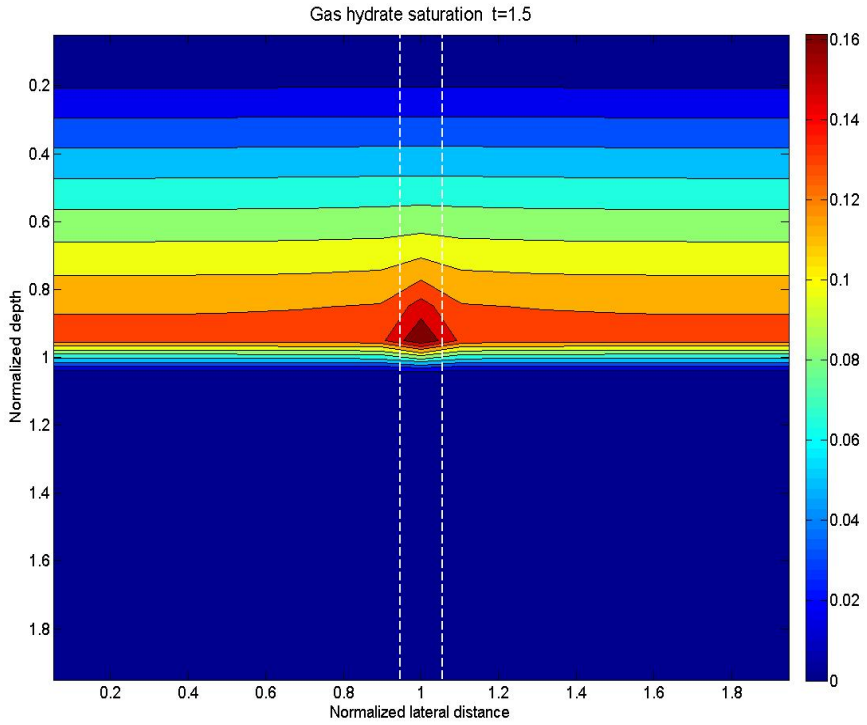

Figure: Gas hydrate saturation contours at dimensionless time t=1.5 for a stationary fracture

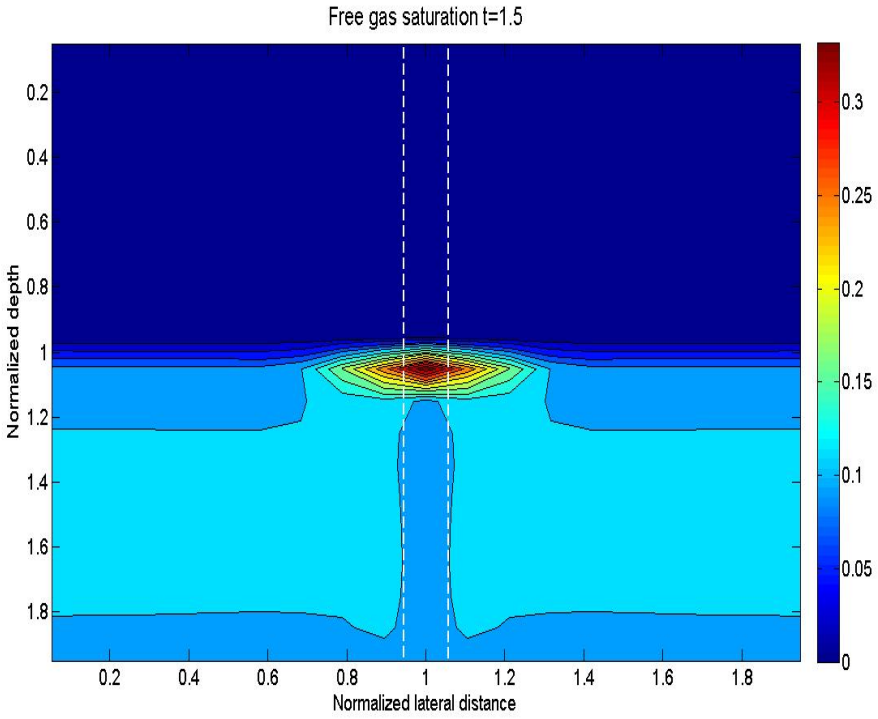

Figure: Free gas saturation contours at dimensionless time t=1.5 for a stationary fracture

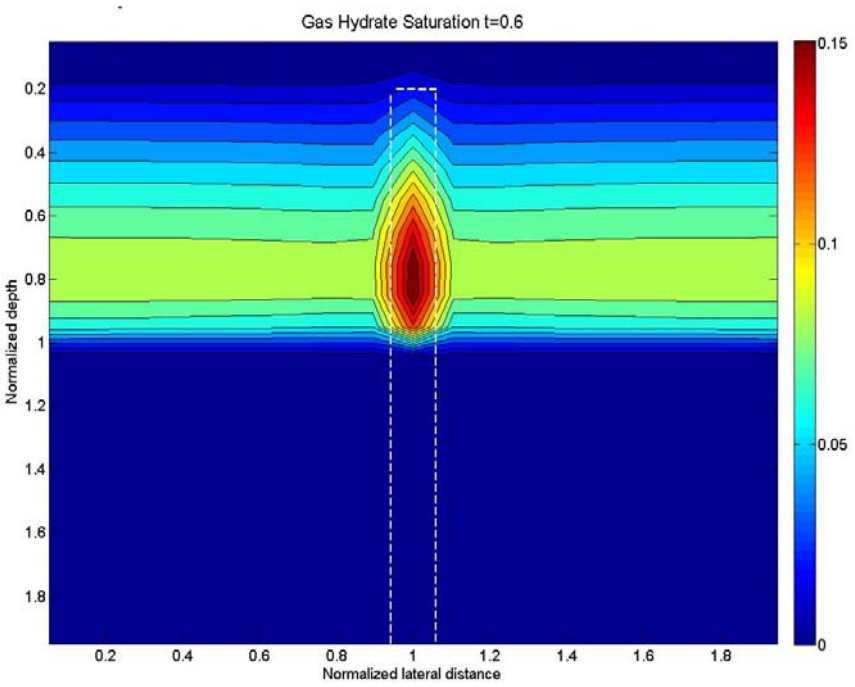

Figure: Gas hydrate saturation contours at dimensionless time t=0.6 for a moving fracture

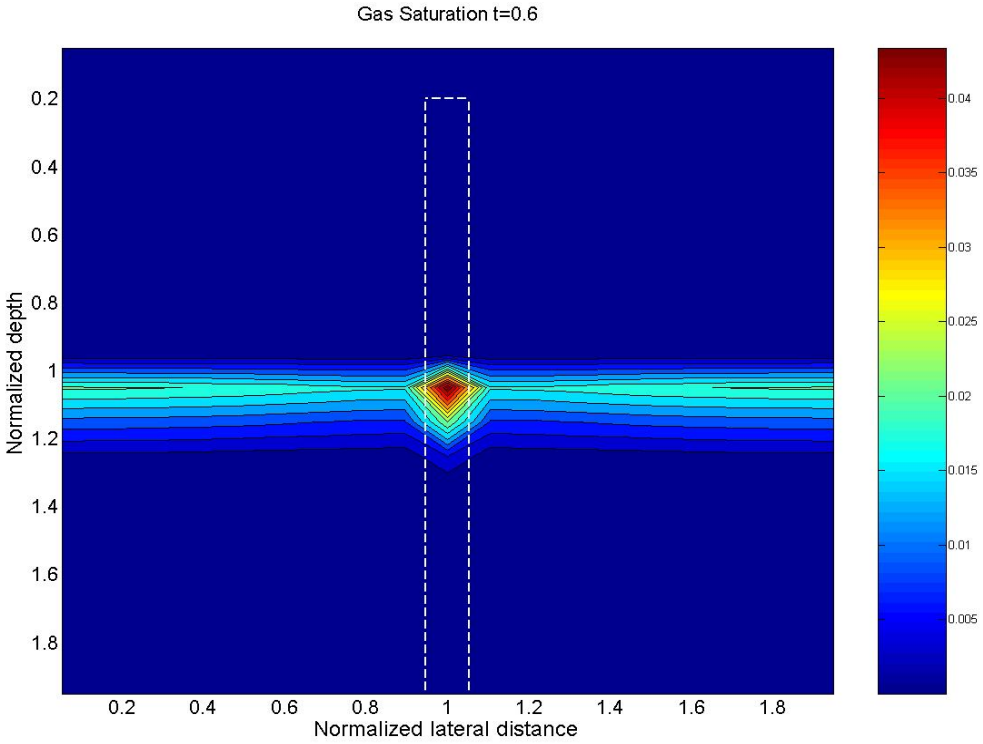

Figure: Free gas saturation contours at dimensionless time t=0.6 for a moving fracture

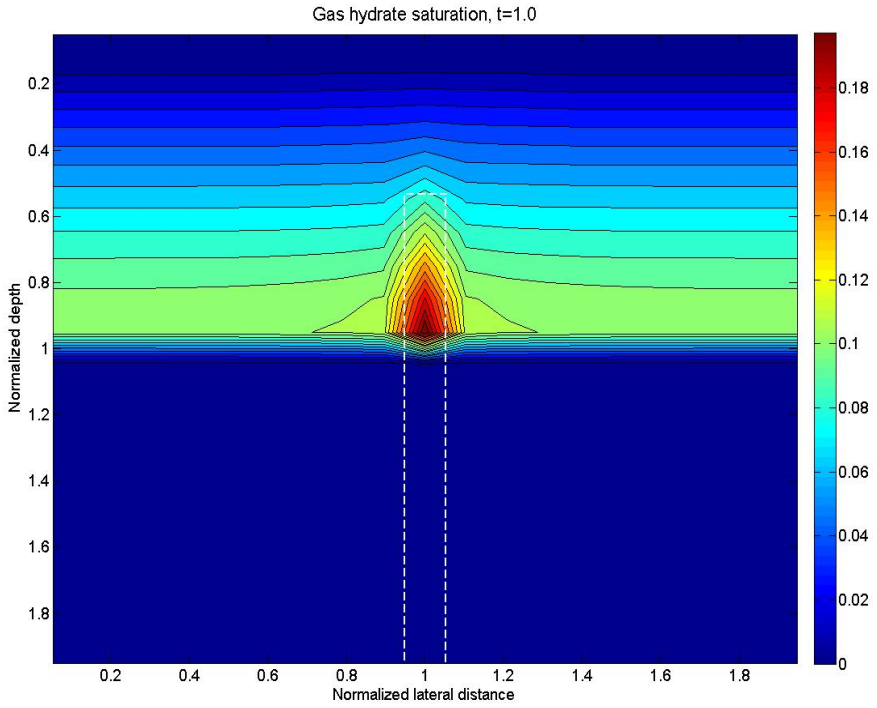

Figure: Gas hydrate saturation contours at dimensionless time t=1.0 for a moving fracture

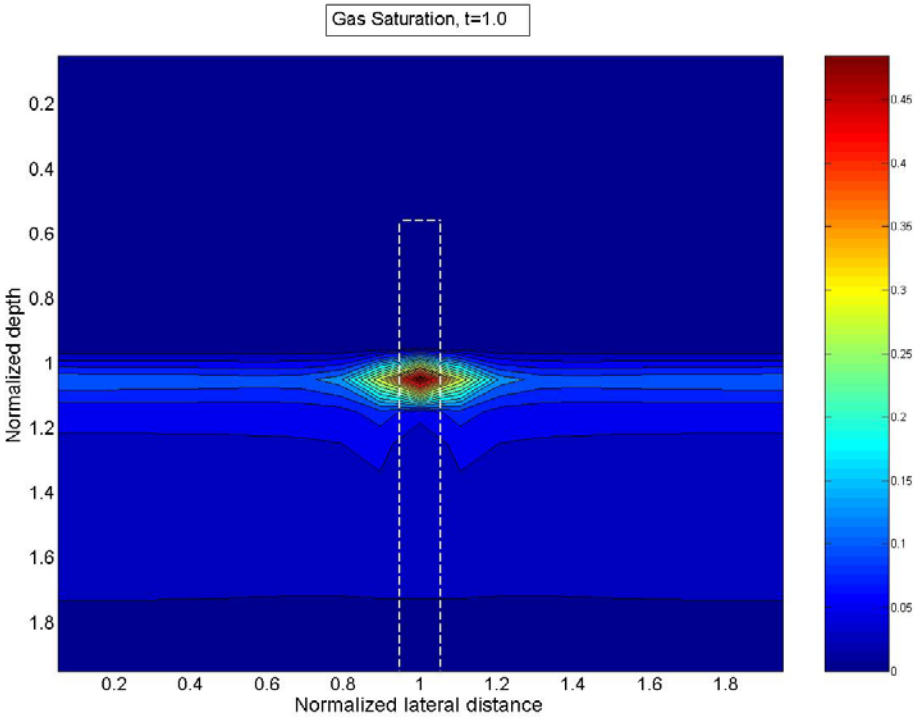

Figure: Free gas saturation contours at dimensionless time t=1.0 for a moving fracture

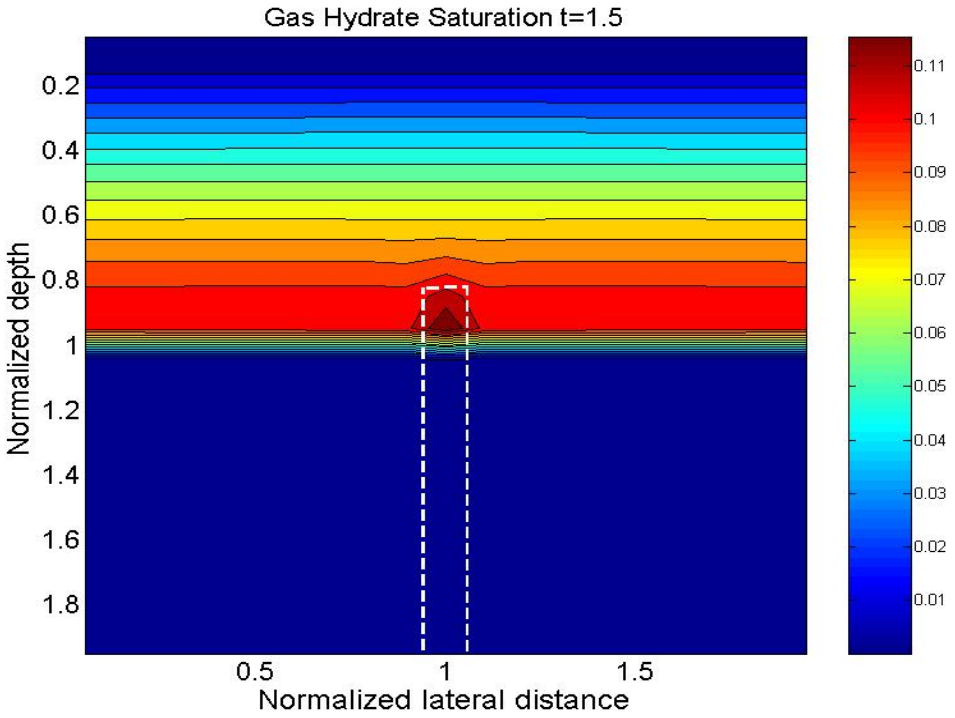

Figure: Gas hydrate saturation contours at dimensionless time t=1.5 for a moving fracture

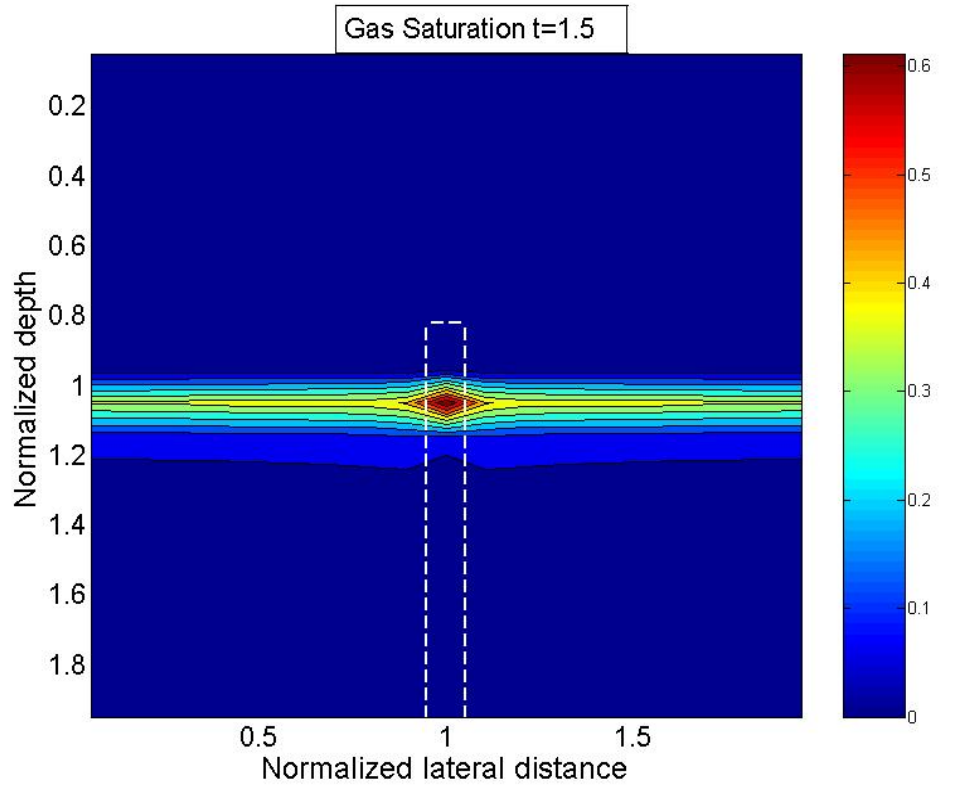

Figure: Free gas saturation contours at dimensionless time t=1.5 for a moving fracture

Gas hydrate systems with dipping sand layers

Our model also comprises of features to simulate high permeability horizontal or dipping sand layers. We start with assigning high permeability to different grid blocks at a particular dip angle as shown below. Similar to the fracture case, the sand layer is assigned 100 times higher permeability than the surrounding clay matrix. The downward movement of this sand layer and transient hydrate and gas saturations are recorded in time. The physical domain for all the simulation is z ϵ [0,2] and x ϵ [0,10]. The parameters remain same as the fracture case mentioned above.

In our case, we simulate a case with high dip angle extending up to middle of our simulation domain. Gas hydrate and free gas saturation contours are shown in figure 13. The plot shows significant hydrate concentration within the sand layer. The focused fluid flow in high permeability sand layer is evident from the results shown. A set of dashed line show the location of sand layer which move down due to sedimentation. Free gas is also focused within the sand layer. We also observe uniform hydrate saturation along the lateral direction when the sand layer exits the system.

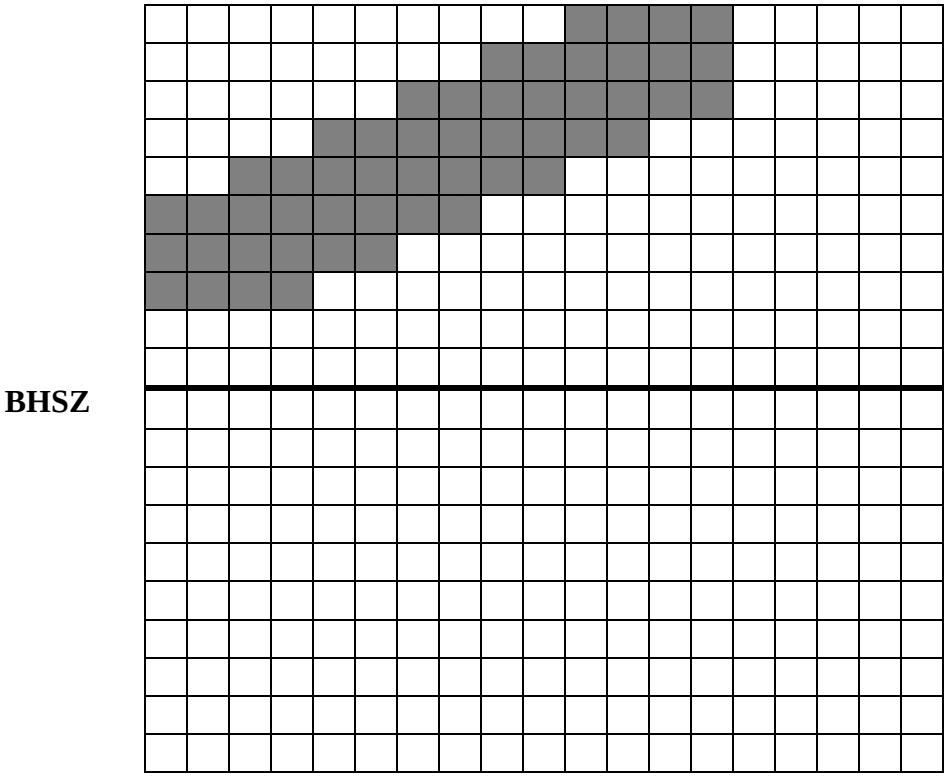

Figure 12: The permeability map schematic representing high permeability sand layers 100 times greater than the surrounding clay sediments

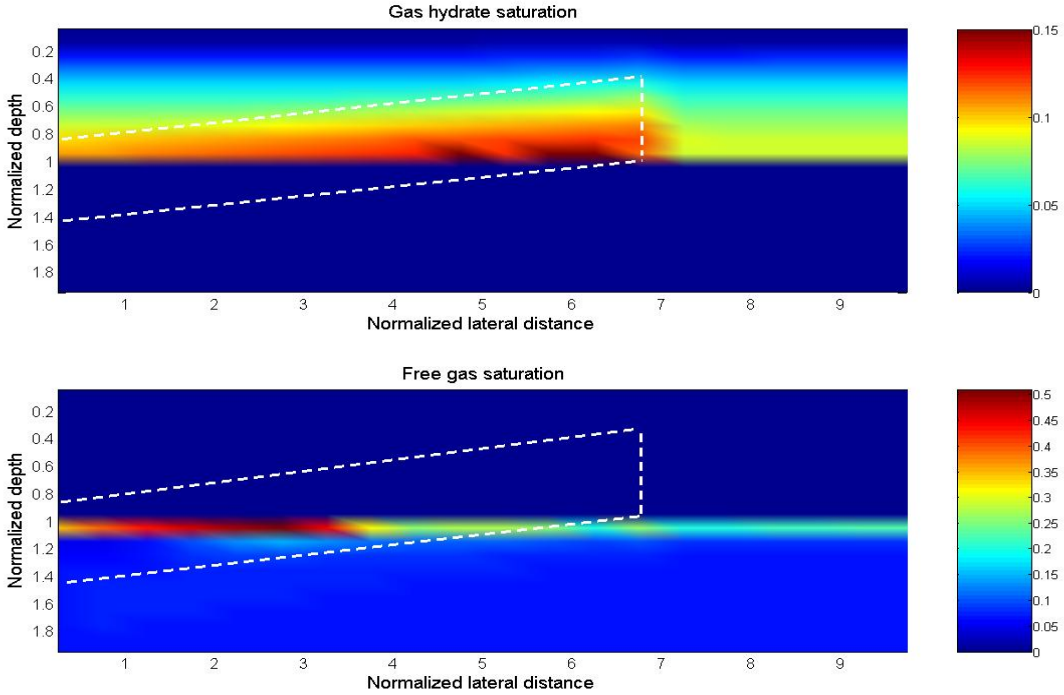

Figure 13: Gas hydrate and free gas saturation contours at dimensionless time t=1.25 for dipping sand layers. Dashed lines show position of the sand layer within low permeability clay matrix

Conclusions

A generalized dimensionless 2-D model has been developed to simulate gas hydrate and free gas accumulation in marine sediments over geologic timescales. We have incorporated heterogeneity in the form of fractures and high permeability sand layers in our model. All this was achieved by just considering biogenic sources in the model. We can expect more gas hydrate saturations by incorporating external upward flux in our model.

Future Work

We will also study the fluid flow direction with the help of quiver plots. This will help us to understand the direction of fluid flux. The focused flow was modest because the ratio of vertical to horizontal permeability (k_v/k_h) was taken to be unity. So, we need to use a more realistic ratio to enable higher values of saturation of hydrate within the conduit. We also wish to model realistic geologic systems with our code. Effect of different parameters, combination of different heterogeneities, with fracture networks have been planned as future work.

References

Bhatnagar G., PhD. Thesis (2008), Accumulation of gas hydrates in marine sediments, 10, p 192-236

6.3. Compositional Effect

Natural gas in the sediments may contain many kinds of gases. Thus compositional effect should be considered if natural gases play important roles in the formation of gas hydrates. In the following work, we focus on the CH_4-C_3H_8-H_2O hydrate system as an example. The effects of propane on the hydrate formation condition and on hydrate distribution, are studied. D. Sloan's CSMGem program is used to obtain data.

An example saturation calculation will be presented in the end of the following work. The purpose of this example calculation is to demonstrate the possibility of gradual change of saturations with distance in sediment. The calculation is based on constant composition, whereas compositions will change during fluid migration in realistic cases.

Denote the overall molar fraction of species *i* as:

$$x_i = \frac{n_i}{n_{CH4} + n_{C3H8} + n_{H2O}}$$, *i* = CH_4, C_3H_8, H_2O.

where n_i is the amount of species *i* in the system (unit: mol), *i* = CH_4, C_3H_8, H_2O.

The water free molar fraction of species *i* is denoted as:

$$x_i^{wf} = \frac{n_i}{n_{CH4} + n_{C3H8}} = \frac{x_i}{x_{CH4} + x_{C3H8}}$$, *i* =C H_4, C_3H_8.

(1) Incipient Hydrate Formation Condition and Phase Regions

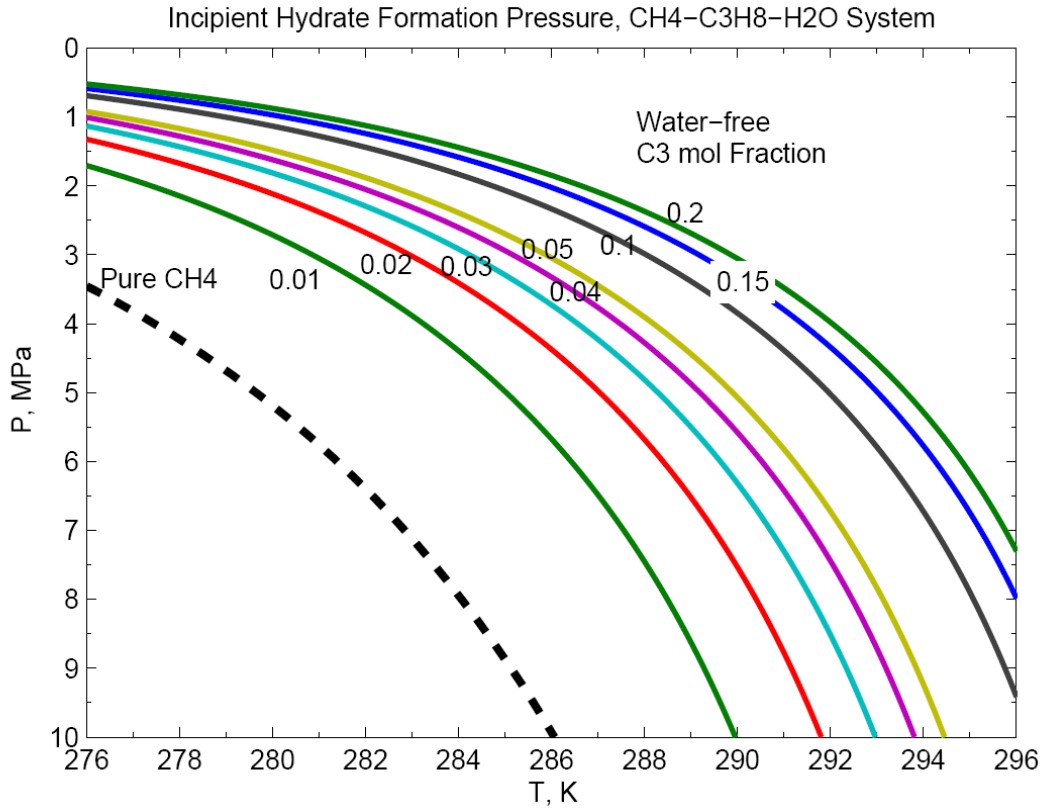

Fig. 6.3-1. Incipient Hydrate Formation Pressure of the CH_4-C_3H_8-H_2O System. Water is in excess. The data labeled for each curve, are the water-free propane molar fractions. The black dash curve, is for the pure CH_4-H_2O system (i.e. water-free propane molar fraction = 0).

Fig. 6.3-1 shows the incipient hydrate formation pressure of the CH_4-C_3H_8-H_2O System. It can be found out that for x_{C3H8}^{wf} = 0.01, the incipient hydrate formation pressure differs very much from that for the pure CH_4 system (i.e., x_i^{wf} = 0).

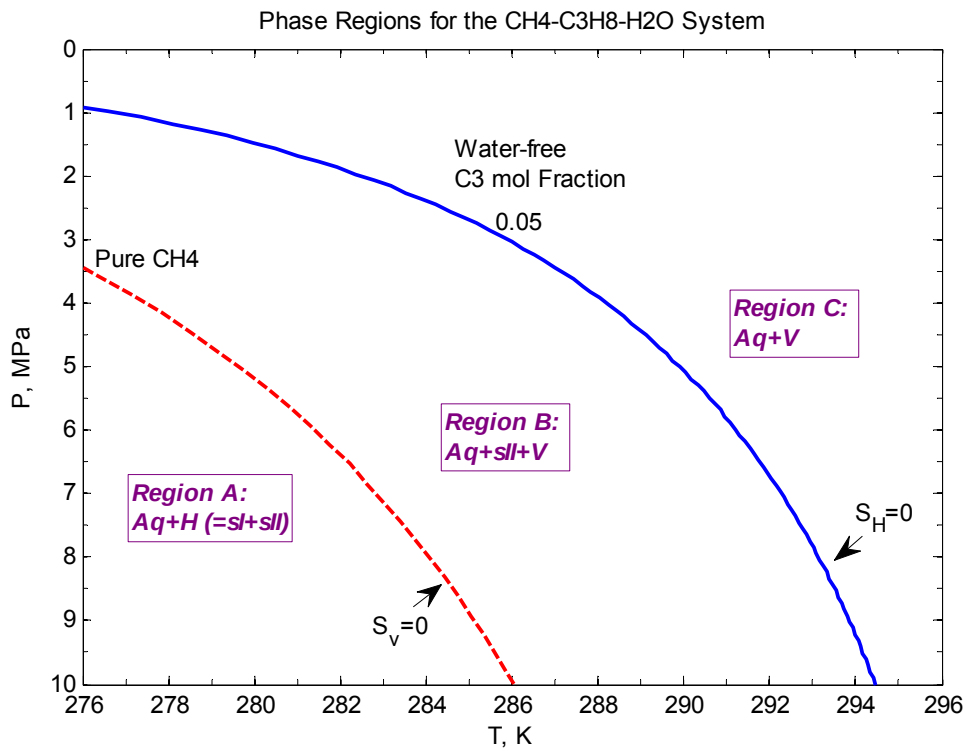

Fig. 6.3-2. Phase Regions of the CH_4-C_3H_8-H_2O System (water-free propane molar fraction is 0.05). Water is present in excess. The red dash curve is the incipient hydrate formation pressure for the pure CH_4-H_2O system. There are 3 phase regions: Region *A, B, C*. Region *A*: *Aq + Hydrate* (= *sI + sII*); Region *B*: *Aq + sII + V*; Region *C*: *Aq + V*. The red dash curve, and the blue solid curve, are boundaries for S_v=0 and S_H=0, respectively.

Fig. 6.3-2 presents the phase regions of the CH_4-C_3H_8-H_2O System (x_{C3H8}^{wf} is 0.05). 3 phase regions are marked in the figure. In Region A, both sI and sII hydrates are stable, while in Region B and C, sI is not stable. In Region B, sII is stable, while in Region C, sII hydrate is not stable. Therefore, in Region B, 3 phases can co-exist: Aq, H, and V. The boundaries for S_v=0 and S_H=0 are marked in the Fig. 6.3-2.

(2) Gradual Phase Transition (i.e. Saturation Change) in Sediment

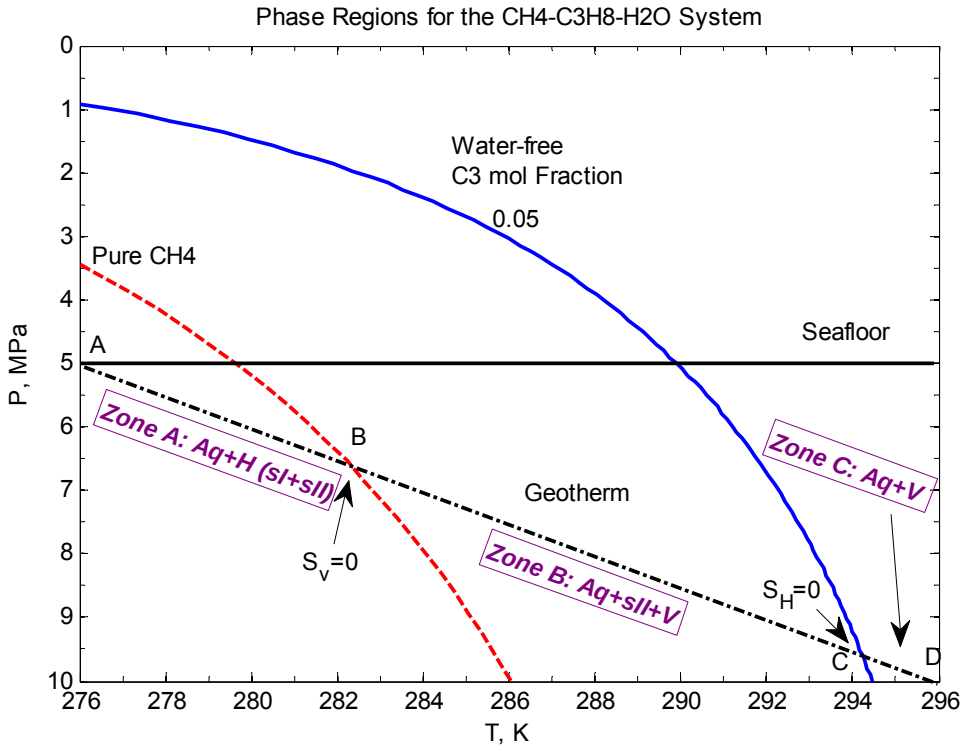

Fig. 6.3-3. Different zones of sediments of a CH_4-C_3H_8-H_2O System (water-free propane molar fraction is 0.05). The Geotherm curve is shown as the black dash-dot curve. There are 3 zones of sediments along the geotherm curve. Zone *A* (Line segment *AB*): *Aq + Hydrate* (= *sI + sII*); Zone *B* (Line segment *BC*): *Aq + sII + V*; Zone *C* (Line segment *CD*): *Aq + V*. Points *B* and *C*, are boundaries for S_v=0 and S_H=0 in the sediment, respectively.

In Fig. 6.3-3 an example geotherm curve in sediment is considered. It can be found out that three different phase zones should exist in the sediment along the geotherm curve, due to the 3 different phase regions described in Fig. 6.3-2. Zone *B* is a special one: 3 phases, *Aq + H (sII) +V*, co-exist. The boundary for S_v=0 in the sediment is the point B in Fig. 6.3-3, while that for S_H=0 is the point C. It's obvious that Zone B (Line *BC*) is a phase-transition-zone corresponding to the boundary of S_v=0 to that of S_H=0. Line BC in Fig. 6.3-4, around 300 m in spatial distance, is definitely very long. Such a gradual change of saturations within a long distance, may result in gradual change of sediment acoustic properties, and further induce weak BSR or even absence of BSR. An example calculation can demonstrate the possibility of such kind of gradual saturation change, as shown in Fig 6.3-4.

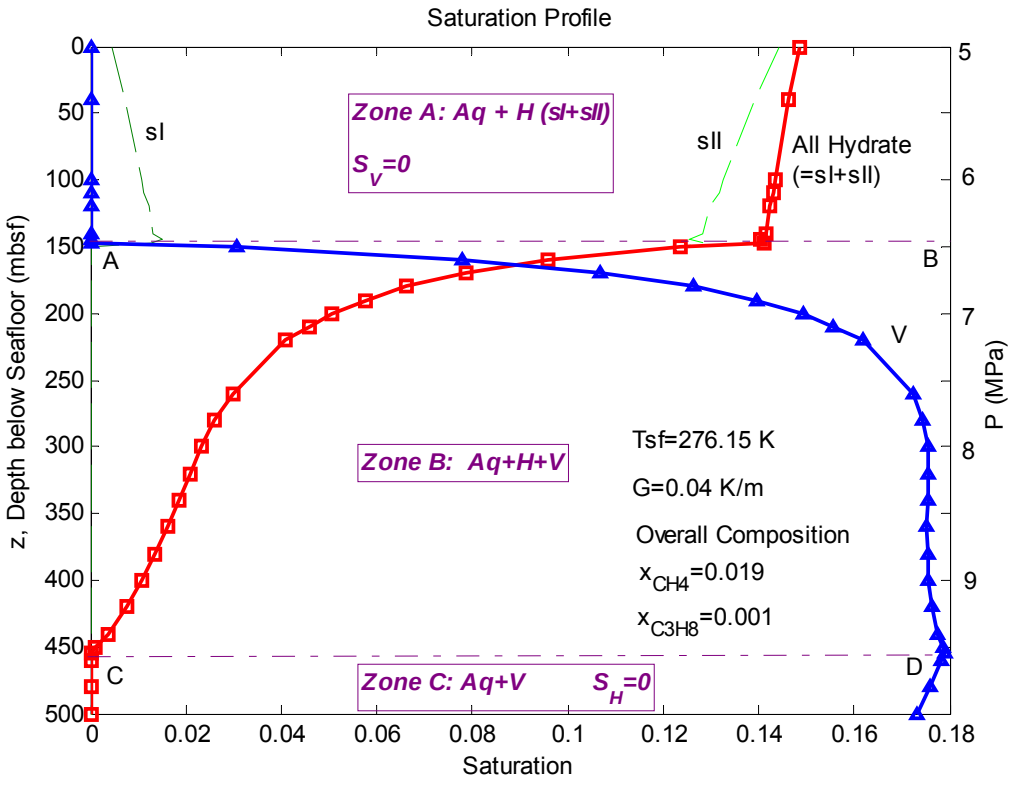

Fig. 6.3-4. An example calculation of a CH_4-C_3H_8-H_2O System (water-free propane molar fraction is 0.05; Overall composition x_{CH4}=0.019, x_{C3H8}=0.001, x_{H2O}=0.98). Assume: The overall composition is the same in the spatial domain. There are 3 zones of sediments in the domain. Zone A: *Aq + Hydrate* (= *sI + sII*); Zone B: *Aq + sII + V*; Zone C: *Aq + V*. Dash-dot line *AB* and *CD*, are boundaries for S_v=0 and S_H=0 in the sediment, respectively. Red solid curve and blue solid curve are saturation profiles for All Hydrate (=sI + sII), and for Vapor, respectively. Seafloor temperature T_{sf} = 276.15 K. Geothermal gradient G= 0.04 K/m. Pressure is marked on the right side.

An example calculation of a CH_4-C_3H_8-H_2O System is presented in Fig. 6.3-4. Here are the conditions and assumptions applied:

(1) Water-free propane molar fraction is 0.05; Overall composition x_{CH4}=0.019, x_{C3H8}=0.001, x_{H2O}=0.98.
(2) Overall composition is constant in the spatial domain.
(3) Seafloor temperature T_{sf} = 276.15 K. Geothermal gradient G= 0.04 K/m.
(4) Seafloor Pressure P_{sf}=5 MPa.

As is well known, there is a sharp phase transition in the CH_4-H_2O hydrate system, which is the basis for BSR. However, for a CH_4-C_3H_8-H_2O System, in Zone *B* in Fig. 6.3-4, from z=147.5 mbsf (Line *AB*) to z= 450 mbsf (Line *CD*), the S_H decreases gradually from 14.1% to 0%, while S_V increases gradually from 0% to 17.9%. Zone *B* is a phase transition zone, in which 3 phases (Aq+H+V) co-exist, and saturations change gradually.

A gradual saturation change will result in the gradual change of acoustic properties with increase in depth, and consequently, very possibly induce a weak BSR, or even absence of BSR.

Conclusion

(1) For the CH_4-C_3H_8-H_2O hydrate system, the incipient hydrate formation conditions are presented. There is a big difference for the incipient hydrate formation condition of the CH_4-C_3H_8-H_2O hydrate system, from that of the CH_4-H_2O hydrate system, even when the water-free-propane molar fraction is only 0.01.

(2) 3 different phase regions are described for different *P*-*T* conditions. As shown in Fig. 6.3-2. Region B is especially important, because Aq, H (sII), V can co-exist. Therefore, in the sediment, 3 zones can be present. Zone B, is the phase-transition-zone, because Aq, H (sII), V co-exist, and S_H and S_v change gradually.

(3) The result of an example saturation calculation of the CH_4-C_3H_8-H_2O hydrate system in the sediment is presented in Fig. 6.3-4. It's successfully demonstrated that gradual change of S_H and S_v within a long spatial distance (~300 m) is possible. Such a gradual change of saturations, may result in gradual change of acoustic properties, and induce weak BSR or even no BSR.

Future Work

The work presented in this report is based on constant composition in sediment as an example. In real situations, the composition in spatial domain is not constant, but dependent on various kinds of factors, such as the fluid flow, diffusion, and phase transformation. Therefore, compositional fluid migration simulation with consideration of fluid flow, diffusion, phase transformation, will be carried out to compute realistic compositions and saturation profiles. The acoustic impedance and seismic reflection will be computed from the saturation profile.

Task 7: Analysis of Production Strategy

J. Phirani & K. K. Mohanty, University of Houston

In this work, we are considering injection of warm water and depressurization for production from Class 2 hydrate reservoirs. The source of warm water could be a nearby oil reservoir or an underlying water aquifer. Gas production from a hydrate reservoir is studied through numerical simulation.

The numerical model used is a finite-volume simulator that takes into account heat transfer, multiphase fluid flow and equilibrium thermodynamics of hydrates. Four components (hydrate, methane, water and salt) and five phases (hydrate, gas, aqueous-phase, ice and salt precipitate) are considered in the simulator. Water freezing and ice melting are tracked with primary variable switch method (PVSM) by assuming equilibrium phase transition. Equilibrium simulation method is used here because kinetics of hydrate formation and dissociation are relatively fast in the field-scale. This simulator has been validated against several other simulators for the problems in the code comparison study conducted by US DOE.

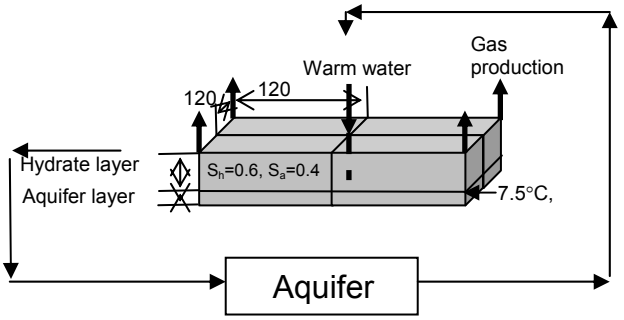

Figure 7-1: Domain considered for the base case

The objective of this study is to identify optimum production strategies for gas production from Class 2 hydrate reservoirs through numerical simulation. The domain selected as the base case is a quarter five-spot of size 120m x120m x10m (Figure 7-1). Initial temperature and pressure are assumed to be 7.5°C and 9MPa, respectively, which lie in the hydrate stable zone. The bottom 2m of the domain is an aquifer layer (S_A=1.0) and the top 8m is a hydrate layer with a hydrate saturation, S_H of 0.6 and aqueous saturation, S_A of 0.4. There is no heat and mass transfer though the side boundaries due to symmetry. There is only heat transfer, but no mass flow through the top and bottom boundaries due to impermeable shale layers. The effect of injection temperature, injection pressure and production well pressure on gas and water production is studied. The

saturation histories encountered in these simulations will be modeled at the pore scale for transport properties.

RESULTS

Simulations were run for different injection pressures, injection temperatures and production pressures for 3000 days and total production of gas was compared for the above parameters.

For the case of no injection, the dissociation is due to pressure falling below the hydrate stable pressure due to depressurization at the production well. The heat of dissociation comes from surroundings, decreasing the temperature of the reservoir. Ice starts forming if the pressure goes below quadruple point pressure. After all the hydrates dissociate, the temperature again starts rising by the heat from surroundings.

For the case of warm water injection, the pressure of injection has to be higher than the reservoir pressure for the hot water to go in. The temperature rise is higher for higher temperature and higher injection pressure (injection flow rate increases). But if injection pressure is high the average pressure in the reservoir increases, slowing the dissociation of hydrates (and even formation of additional hydrates) before the warm water reaches a certain region. If production pressure and temperature are both high, the rate of production of gas increases. The total production of gas also depends on the production pressure, and for different production pressure the optimum injection conditions vary.

Figure 7-2 shows total production for the production well pressure of 2MPa. The injection temperature was kept constant at 20C and injection pressure was varied. The results were compared against the no injection or depressurization only case. When warm water is injected at a higher pressure but at a relatively low temperature (20C in the present case) the gas production rate decreases with increasing injection pressure. This is because the average pressure of the reservoir domain increases; dissociation of hydrate slows down. In case of 5MPa of injection pressure, the total production of gas increases because water occupies some pore space that would have been occupied by gas during depressurization. At higher injection pressure the hydrate dissociation is not complete in 3000 days. For low temperature water injection, only depressurization seems to be better than warm water injection.

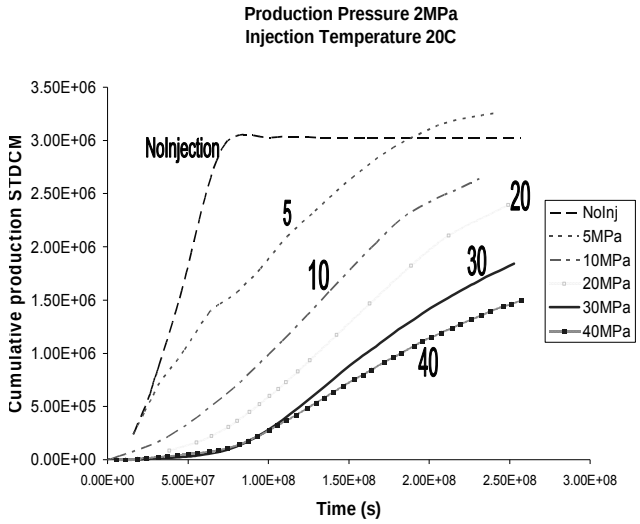

Figure 7-2: Cumulative production of gas with varying injection pressure, 20°C of injection temperature and 2MPa of production pressure

Figure 7-3 shows the cumulative production of gas when production well pressure is kept at 4MPa and injection temperature is 80°C. The injection pressure is varied. In this case, only depressurization is slow and does not dissociate all the hydrates present in 3000 days. With increasing injection pressure the gas production rate increases. With an injection water of 80°C, as the injection pressure increases more of the reservoir gets to this high temperature which helps in hydrate dissociation.

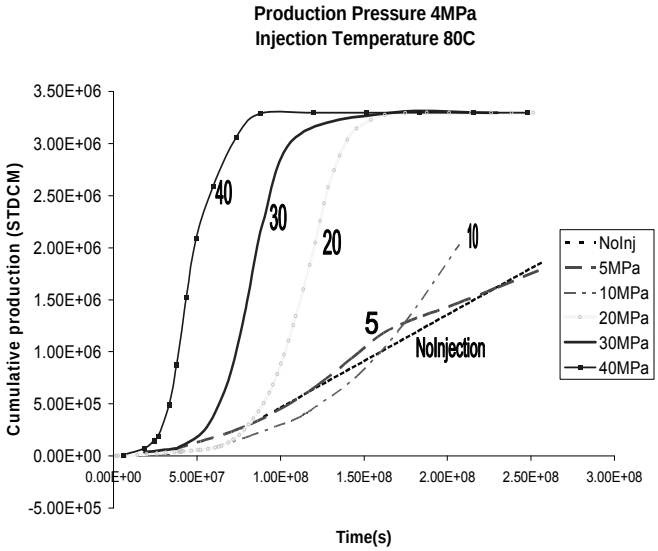

Figure 7-3: Cumulative production of gas with varying injection pressure at 80°C of injection temperature and 4MPa of production pressure.

If injection temperature is in medium range (50°C) then injection pressure and production pressure play an important role. Figure 7-4 and 7-5 are plots for

2MPa and 4MPa of production pressure, respectively, at 50°C of injection temperature with varying injection well pressures. If Injection pressure rises from 5MPa to 10MPa the production almost remains same for the case of production pressure 2MPa but decreases drastically in the case of production pressure 4MPa. This can be attributed to higher average pressure in the reservoir domain which hinders hydrate dissociation. In case of injection pressure of 30MPa and 40MPa the total production and rate of production increases (Figure 7-4 and 7-5), though initial rate of production falls due to increase in average reservoir pressure which assists hydrate formation while temperature is still not high. The gas production rate is non-monotonic with the increase in injection pressure.

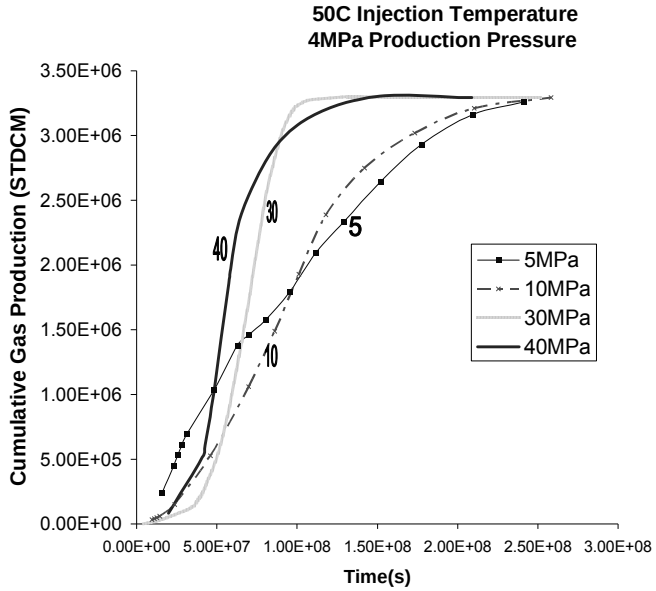

Figure 7-4: Cumulative gas production with varying injection pressure and 2MPa of production pressure and 50°C of injection temperature.

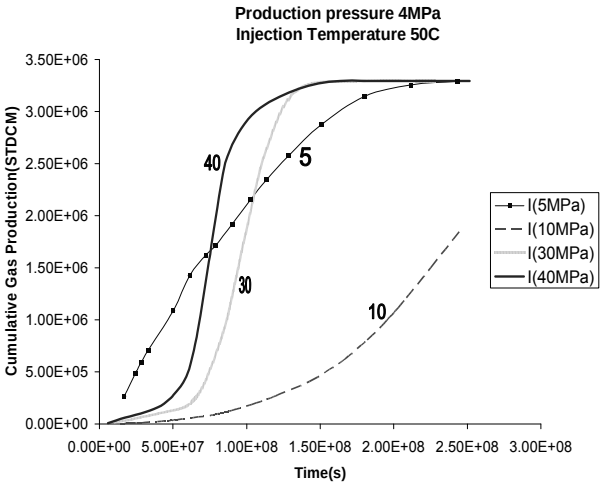

Figure 7-5: Cumulative gas production with varying injection pressure and 4MPa of production pressure and 50°C of injection temperature.

CONCLUSIONS

The production well pressure, injection temperature and pressure play an important role in the production of gas from hydrate deposits. For high injection temperature, the higher pressure increases the flow of warm water (heat) in the reservoir making the production rate faster, but if injection temperature is not high then only depressurization is the best method of production. At intermediate injection temperature, the production rate changes non-monotonically with the injection pressure. These parameters should be chosen carefully to optimize recovery and recovery rate of gas. This paper addresses a very simple homogeneous domain. Realistic reservoirs would have heterogeneity in sediments as well as hydrate distribution, which need to be taken into account. Models are being developed in Dr. Hirasaki's group to address the variation in hydrate saturation in marine sediments.

Next Quarter:

Pore-scale model to estimate the transport properties.

Task 8: Seafloor and Borehole Stability

Approach

We are using published literature to constrain the mechanical properties of hydrate bearing sediments to understand deformation, flow, and strength properties that affect regional seafloor stability and local borehole stability. This includes culling the literature to assess what data have been compiled, the method of measurement, and identifying where strengths and gaps exist. Secondly we are running laboratory experiments on fine-grained materials from hydrate settings but in the absence of hydrate. These experiments will set the baseline parameters (permeability, compressibility, strength) for model inputs that are the modified according to hydrate saturation. We are also coupling the physical properties into basin-scale fluid flow models that simulate sediment accumulation and conditions that can lead to slope instability.

Results and Discussion

The literature search is complete. We have worked with other hydrate researchers to be as complete as possible and make sure we have digital reprints of the papers and reports. We have begun reviewing the papers and compiling data sets. After a three-day workshop in Atlanta, GA, three key gaps have been identified: (1) physical properties of fine-grained materials at low (<40%) hydrate saturation; (2) relative permeability measurements for gas and water in hydrate bearing sediments; and (3) consistent measurements of strength in hydrate bearing sediments. Rice is taking the lead in (1) and we are working with MIT to develop a technique to address this issue by working with ice-water-sediment systems in existing infrastructure. We will be submitting an external proposal to fund the experiments. Lawrence Berkeley National Laboratory is taking the lead on (2) with their experimental set-up. We hope to have some preliminary results by the OTC conference in May to include in our database. Issue (3) is of greater scale and we are working on the best way to solve it as it involves integrating data and methods from different labs; and the methods have a very large impact on the strength. We (Rice, LBNL, GATech, USGS) have started a physical properties review paper based on the existing data.

We have a new sample procedure for permeability experiments that will let us make measurements of horizontal and vertical permeability in sediments. This will provide useful constraints on permeability anisotropy for inputs into basin-scale models that have shown anisotropy and heterogeneity are important aspects of hydrate distribution and saturation (Task 6).

Our basin-scale models of fluid flow have been coupled to a slope stability calculation that we are testing in the absence of hydrate. Preliminary tests are able to predict when slope failures will exist under different pore pressure regimes and seafloor slopes. In summer 2008, I plan to have Justin Stigall (Earth Science graduate student, Task 8) work with Sayantan

Chatterjee (Chemical & Biomolecular Engineering graduate student, Task 6) to implement the stability calculations in the two-dimensional models that couple sedimentation, consolidation, fluid flow, and hydrate accumulation.

Milestone Progress

8.1a Collection of data (05/08): We have compiled an extensive literature database encompassing flow, strength, and deformation properties. We are cataloging the literature in EndNote. This collection should be complete on target.

8.1b Complete database (1/09): As we are cataloging the data, we are identifying the key datasets that exist and the key measurements that are missing. We have made contact with other DOE-funded groups (USGS-Woods Hole, Georgia Institute of Technology, Lawrence Berkeley National Laboratory) to address how key gaps might be filled with existing infrastructure and facilities. The final database will include a summary of existing data and also a plan for filling the data gaps. The task is on target for 01/09.

8.2a Link database with models (08/08): We will provide Tasks 6 and 7 with the data we have by 08/08 to help guide and/or interpret simulations.

8.2b Add sediment stability to models (10/08): Standard slope stability calculations have been implemented in a hydrogeologic model and are being tested in one- and two-dimensions in the absence of hydrate (i.e., sediment-water systems only). This allows us to validate the models for known scenarios. After we complete testing (05/08) we will work the Tasks 6 and 7 to see how these calculations can be implemented in the existing models. The task is still on target for completion by 10/08.

8.2c Conditions for (in)stability (09/09): This milestone can be addressed once we complete Milestone 8.2a, which is on target.

Presentations

Daigle, H., Dugan, B., Nuclear Magnetic Resonance Permeability Estimation in Fine-Grained Sediments, Rice University Consortium on Processes in Porous Media, 26 March 2008.

Abstracts

Daigle, H., Dugan, B., in review, Extending Nuclear Magnetic Resonance Data for Permeability Estimation in Low-Permeability Sediments, 2008 Schlumberger Information Solutions Global Forum, Paris, France, 6-9 October 2008.

Additional Hydrate Related Work

Through with the Rice Hydrate grant through DOE, I have maintained active involvement in the Gulf of Mexico Gas Hydrates JIP to locate drilling targets and methodologies. From these interactions, I have access to seismic and log data

from the Gulf of Mexico that we (Rice) intend to use to make hydrate saturation predictions for the previously studied (Atwater Valley, Keathley Canyon) and to-be studied (Alaminos Canyon, Green Canyon, Walker Ridge). Also I have made offered to help in the safety analysis for the upcoming JIP drilling by doing a pore pressure prediction. Emrys Jones (Chevron) has recently introduced me to Rana Roy (Chevron) to follow up on the pressure analysis.

Task 9: Geophysical Imaging of Gas Hydrate and Free Gas Accumulations

For this task in particular, and others in general, we have successfully initiated collaboration with National Institute of Oceanography (NIO), India. We intend to demonstrate geophysical imaging with multichannel seismic data from the Krishna-Godavari (K-G) basin in the Indian east coast. NIO scientists are tentatively scheduled to visit Rice University in the first week of June.

Though Priyank Jaiswal has not started working on the gas hydrate project officially, he is helping NIO in preliminary processing of the selected seismic line and thus is working towards subtask 9.1. The results of the preliminary processing will be shown at Rice University by the NIO scientists during their scheduled visit.

It is estimated that Priyank Jaiswal will start working on the project directly as a Post Doc sometimes in summer.

Subtask 9.1: Preliminary processing and inversion of seismic data.

Seismic data has been identified and is currently being processed at NIO, India with Priyank's remote involvement. The identified seismic line (Figure attached) has three inline wells all of which were drilled in 2001. The drilling was based on BSR signatures that appear to be similar at the well locations but the recovered hydrate concentration was found to be varying.

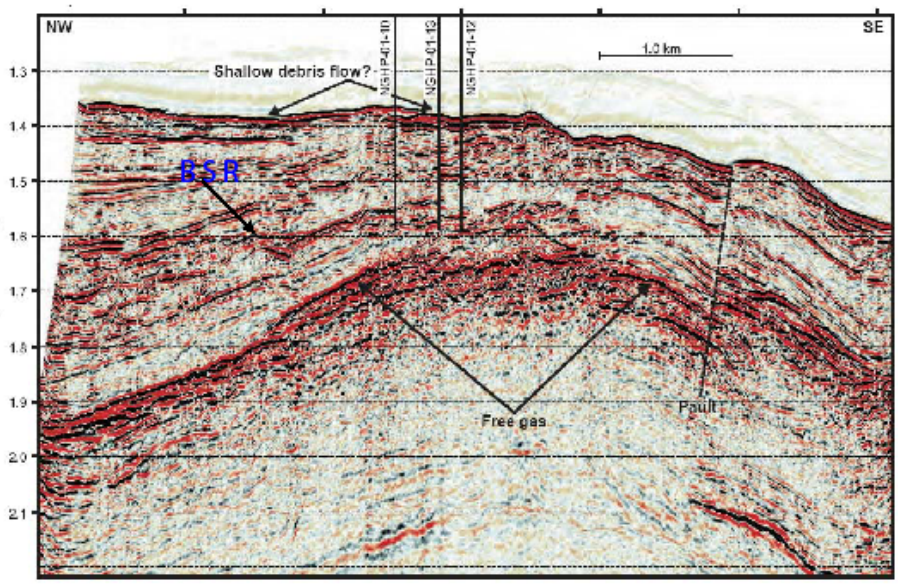

Seismic data from the K-G basin showing NGHP drill sites 10, 13, and 12. Site 12 had massive hydrate contents while 10 and 13 did not.

COST PLAN / STATUS					
	Phase 1	Phase 2: Year 1 (June 2007 - May 2008)			
Baseline Quarter Reporting		7/1/07 TO 9/30/07	10/1/07 TO 12/31/07	1/1/08 TO 3/31/08	4/1/08 TO 6/30/08
Baseline Cost Plan (SF-424A)					
Federal Share	$ 3,624	$ 80,003	$ 80,003	$ 80,003	$ 80,003
Non-Federal Share	$ 1,004	$ 28,653	$ 28,653	$ 28,653	$ 28,653
Total Planned	$ 4,628	$ 108,656	$ 108,656	$ 108,656	$ 108,656
Cumulative Baseline Cost	$ 4,628	$ 113,284	$ 221,940	$ 330,596	$ 439,252
Actual Incurred Cost					
Federal Share	$ 3,082	$ 59,364	$ 20,610	$ 55,903	
Non-Federal Share	$ 1,091	$ 18,616	$ 33,647	$ 27,599	
Total Incurred	$ 4,173	$ 77,980	$ 54,257	$ 83,502	
Cumulative Costs	$ 4,173	$ 82,153	$ 136,410	$ 219,912	
Variance (plan-actual)					
Federal Share	$ 542	$ 20,639	$ 59,393	$ 24,100	
Non-Federal Share	$ (87)	$ 10,037	$ (4,994)	$ 1,054	
Total Variance	$ 455	$ 30,676	$ 54,399	$ 25,154	
Cumulative Variance	$ 455	$ 31,131	$ 85,530	$ 110,684	

Milestone Plan/Status

Task	Milestone: Status and Results	Date	Status
5. Carbon inputs and outputs to gas hydrate systems	5.1a Measure iodine in sediments We have measured iodine concentrations in pore waters from several gas hydrate systems. The analyses are completed and we are writing the results over the summer.	12/07	1/08
	5.1b Constrain C_{org} inputs from iodine We will measure the content and isotopic composition of organic carbon and carbonate in sediment from cores of several gas hydrate systems. We have collected most of the samples, although plan to visit the ODP repository (College Station) in late spring or early summer to collect additional samples. Most analyses will be done this summer, although we anticipate examination of a small "trial batch" of samples from the Peru Margin in the next month. Some analyses have been completed; additional ones will be done over the summer.	10/08	
	5.2a Construct metal profiles in sediments We will measure metal contents in sediment from cores of several gas hydrate systems to constrain past hydrocarbon outputs via anaerobic oxidation of methane (AOM). Because initiation of project funding was slowed, we began some of this work last year with scientists from Japan using samples of opportunity from the Sea of Japan. Some work was published in the fall (Snyder et al., 2007). We plan on submitting a manuscript regarding profiles on the Peru Margin by the end of summer.	12/09	

	5.2b Modeling/integrating profiles We will use the metal and iodine profiles to constrain models for gas hydrate formation. We have discussed data and models but have not begun this work so far.	12/10	
6. Numerical models for quantification of hydrate and free gas accumulations	6.1 Model development. The recipient shall develop finite difference models for the accumulation of gas hydrate and free gas in natural sediment sequences on geologically relevant time scales.	9/07	1/08
	6.2: Conditions for existence of gas hydrate The recipient shall summarize, quantitatively, the conditions for the absence, presence, and distribution of gas hydrates and free gas in 1-D systems by expressing the conditions in terms of dimensionless groups that combine thermodynamic, biological and lithologic transformation, and transport parameters.	3/07	done
	6.3 Compositional effect on BSR The recipient shall add to the numerical model, developed under this task, a chloride balance and multi-hydrocarbon capability specifically to investigate how hydrocarbon fractionation might affect Bottom Simulating Reflectors (BSRs).	7/07	12/08
	6.4: Amplitude Attenuation and chaotic zones due to hydrate distribution The recipient shall simulate preferential formation of gas hydrate in coarse-grained, porous sediment in 2-D by linking fluid flux to the permeability distribution.	3/09	
	6.5: Processes leading to overpressure The recipient shall quantify, by simulation and summarize by combination of responsible dimensionless groups, the conditions leading to overpressure to the point of sediment failure.	3/08	

	6.6 Concentrated hydrate and free gas The recipient shall, using 2-D and 3-D models, simulate lateral migration and concentration of gas hydrate and free gas in structural and stratigraphic traps.	3/08	
	6.7 Focused free gas, heat and salinity The recipient shall quantify, using 2-D and 3-D model simulations and comparisons to available observations, the factors controlling the process of localized upward migration of free gas along faults and lateral transfer to dipping strata that can lead to chaotic zones and possible accumulations of concentrated hydrate.	9/09	
	6.8 Sulfate profile as indicator of methane flux The recipient shall compute, for systems where data on the sulfate profile is available, the oxidation of methane by sulfate and shall indicate the perceived level of effect on gas hydrate accumulation and the data's value as an indicator of methane flux.	7/07	done
	6.9 Application of models to interpretation of case studies. The models developed in Task 6 will be applied to case studies in the interpretation of each of the other tasks.	6/10	6/10
7. Analysis of production strategy	7.1a Pore scale model development and Hydrate code comparison For this milestone, we will develop pore-scale models of hydrate accumulation by simulation. Our hydrate code will be used to solve a set of problems formulated by the Code Comparison Study group. Our results will be compared with those of other hydrate codes. Should be changed to: 6/08 Reason: The starting date was moved to 6/07 Status: Code comparison study is 80%	1/08	6/08 Code comparison is done.

	complete.		
	7.1b Petrophysical and thermophysical properties of hydrate sediments from pore-scale model For this milestone, we will assume the pore-scale models of hydrate accumulation developed in the last milestone and estimate transport properties as a function of hydrate and gas saturations. Should be changed to: 6/09 Reason: The starting date was moved to 6/07 Status: Have not started	1/09	6/09
	7.2a Modeling of several production strategies to recover gas from marine hydrates Several production strategies would be modelled using the transport property correlations developed in the previous milestone. Optimal strategies will be identified. Should be changed to: 6/10 Reason: The starting date was moved to 6/07 Status: Have not started	1/10	6/10
	7.2b Effect of marine reservoir heterogeneities on production of methane Reservoir heterogeneity anticipated in marine environments (known or determined through other tasks) would be incorporated. Appropriate hydrate distributions, either constrained from experimental data or mechanistic simulations (Task 5) would be used. Sensitivity of gas production to the heterogeneities would be calculated. Should be changed to: 6/11 Reason: The starting date was moved to 6/07 Status: Have not started	12/10	6/10
8. Seafloor and borehole stability	8.1a Collection of data Status: 05/08 (large shift according to	10/07	05/08

	anticipated start date and dispersement of funds to Rice) To achieve this milestone, we will perform a literature and database search of existing geomechanical properties of sediments with hydrate and sediments without hydrate from hydrate settings. This will include laboratory experiments, field data, published results, and unpublished data.		
	8.1c Complete database Status: 1/09 (some shift due to delay of data collection) We will organize the data from task 8.1a into a format that can be easily searched and used by any researchers trying to understand mechanical behavior of hydrate-bearing sediment. We will also identify key gaps in the database for focusing future hydrate research endeavors.	10/08	01/09
	8.2a Link database with models Status: 8/08 From the database we will assess how hydrate saturation affects different geomechanical properties. These relationships can then be input into models of basin development or production.	3/08	8/08
	8.2b Add sediment stability to models Status: 10/08 Standard stability calculations will be coupled with basin scale and production models. The strength characteristics that influence stability will be imported from the relations developed in 7.2a.	10/08	
	8.2c Conditions for (in)stability	9/09	
9 Geophysical imaging of hydrate and free gas	9.1 Preliminary processing and inversion of seismic data. Perform conventional seismic reflection processing, velocity analysis, travel time tomography, and other analyses as deemed appropriate and necessary.	8/08	
	9.2: Final 1-D elastic and 2-D acoustic	8/09	

	waveform inversion. Apply 1-D elastic and 2D acoustic inversions on data obtained from subtask 9.1 to derive determine high-resolution elastic and acoustic properties.		
	9.3: Rock physics modeling. Apply rock physics models to the developed seismic models to estimate hydrate saturation and lithology through application of well log data in conjunction with data from subtask 9.2. For this subtask we shall seek to collaborate with research being conducted under separately funded DOE-NETL projects (DE-FC26-05NT42663 with Stanford University, "Seismic-Scale Rock Physics of Methane Hydrate" and others as applicable).	8/10	

National Energy Technology Laboratory

626 Cochrans Mill Road
P.O. Box 10940
Pittsburgh, PA 15236-0940

3610 Collins Ferry Road
P.O. Box 880
Morgantown, WV 26507-0880

One West Third Street, Suite 1400
Tulsa, OK 74103-3519

1450 Queen Avenue SW
Albany, OR 97321-2198

2175 University Ave. South
Suite 201
Fairbanks, AK 99709

Visit the NETL website at:
www.netl.doe.gov

Customer Service:
1-800-553-7681